Dynamic homogenization of split-ring metamaterials by Floquet-Bloch decomposition

Mohamed Hicham Belyamoun, Olivier Dubrunfaut, and Said Zouhdi*
Laboratoire de Gnie Electrique de Paris, CNRS UMR 8507,
SUPELEC, Univ Paris 06, Univ Paris-Sud, 11 rue Joliot-Curie,
Plateau de Moulon, 91192 Gif-sur-Yvette Cedex, France
(Dated: September 23, 2012)

We apply a novel dynamic homogenization technique to determine the frequency-dependent effective permeability of split-rings arrays. The Floquet-Bloch decomposition of Maxwell equations in this metamaterial is applied when the wavelength is much bigger than the material's period. We replace the inclusion with a closed ring, and numerically simulate the model by nodal finite elements and a reasonable number of tetrahedral mesh elements. Our results show a good agreement with an analytical permeability law for 2D structures. This work also proposes an accurate method to model the magnetic field in the unit cell.

PACS numbers: 42.70.Qs, 78.20.Bh, 41.20.Jb
Keywords: Homogenization, split-ring, magnetic potential, Floquet-Bloch

I. INTRODUCTION

In naturally-occurring materials the refraction index is always positive. However, some artificially microstructured materials can exhibit exotic properties as a negative index[1,2]. The research on these metamaterials, originally pioneered by Veselago[3], has been growing the last years. This interest is mainly driven by the suggested potential applications, including the miniaturization of electromagnetic devices[4] and the realization of subwavelength resolution lenses[5,6].

A periodic artificial material constituted of conducting inclusions distributed in a dielectric matrix could act as a continuous medium with effective constitutive properties, at least in the long wavelength limit. For instance, a material formed by an array of thin metallic wires can have a plasma frequency, hence a negative permittivity, in the microwave regime[7]. In the other hand, magnetic structures with a negative permeability can be obtained by arranging non closed metallic rings in a dielectric host medium. These so called split ring resonators (SRR) has been proposed to limit the absorption of the swiss-roll structure[8] and quickly become the archetypical magnetic component in metamaterials. The majority of the implemented negative index metamaterials being based on different kinds of split-ring arrays, these inclusions benefit from numerous studies to determine the resonance frequency[9,10] and the magnetic field distribution[11,12].

Some methods have been proposed in order to compute the bulk properties for the metamaterials. The retrieval procedure[13] consists in extracting the effective constitutive parameters from the complex reflection and transmission coefficients for a finite metamaterial's thickness. However, this method does not provide significant physical insight into the nature of the artificial material and is subject to multiple branch solutions[14]. Despite it has been greatly improved in several ways[15], it is requiring the full simulation of the periodic structure.

Other methods avoid the heavy computation of S-parameters. As a matter of fact, the computation of the effective parameters could be done with minimum cost if we can take advantage of the structure translational symmetry. Instead of solving the problem over the whole structure, we would only study the symmetry cell. The homogenization[16] approach consists in finding the effective homogeneous medium that approximate best the initial periodic structure. The incident planar wave "sees" the structure as homogeneous when the cell's dimensions are small compared to the wavelength.

Early attempts of homogenization made in the nineteenth century, summarized in Ref.[17], still give inspiration today. The paper of Belov and Simovski[18] discusses the limits of homogenization and proposes an effective permeability as a generalization of the classic Clausius-Mossoti formalism.

In the well-know "field averaging" Ref.[19] and "field summation" Ref.[20], the macroscopic fields are determined via averaging the local field obtained from a EM simulation or analytical calculation in the unit cell with periodic conditions. These approaches are well adapted to study metamaterials with gradient properties[21].

The asymptotic approaches[22,23] can be applied for all structure with complicate shape but the period of the structure is necessarily negligible compared with the relative the free-space wavelength. The periodic unfolding[24] can even model bianisotropic and dispersive metamaterials, unfortunately, it does not apply to resonant inclusions, as the obtained effective parameters are the static ones.

Other methods are based on the Floquet-Bloch analysis[25]. The paper[26] provides frequency dependent bulk parameters, but cannot take into account a finite conductivity. In Ref.[27–29], the problem is solved in a quasi analytical way, which give us a great physical insight. The method developed in Ref.[30] is purely numerical and completely general. It applies to any shape of inclusions while taking into account the spatial dispersion.

The novel numerical method of Ref.[31] allows the homogenization of split-ring arrays with a finite conductiv-

ity. It predicts a negative real part effective permeability in a narrow frequency window. Limited to simple split rings, it is an alternative way to determine numerically the effective permeability, with a low computational cost. In this paper, we describe the numerical implementation of this method and analyze the obtained simulation results.

This work is organized as follows. In Section II, we introduce the single split-ring based metamaterial physical behavior when it interacts with a planar wave. The homogenization process, through the Floquet-Bloch analysis, is inadequate when applied to the full Maxwell equations. We summarize the ingenious solution proposed in[31] to solve this issue. We use the finite elements method to simulate the medium, and we describe the necessary discretization process in Section III. Finally, the simulation results and the comparisons with an analytical law and free-space measurements are drawn in Section IV.

II. HOMOGENIZATION METHOD

A. The split-ring physics

Here, we explain the behavior of an array of split ring resonators when interacting with a planar wave[32–34]. We will take advantage of the translational symmetry and only study the unit cell $\mathcal{C}$, a cube defined by a set $\{V_x, V_y, V_z\}$ of orthnormal vectors. Having the homogenization hypothesis $a \ll \lambda$, the electromagnetic field is supposed uniform over the studied metamaterial. Indeed, we have a split-ring based metamaterial immersed in an uniform monochromatic field $\{\vec{E}, \vec{H}\}$ with a time dependency in $e^{i\omega t}$. The ring $\mathcal{R}$ is "conductive enough" to consider that all the electromagnetic fields are null inside it.

The magnetic excitation $\vec{H}$ induces a flux Φ through the ring. Besides, a strong electric field $\vec{e}$ is created in the air gap region, ensuring an electric continuity by creating an electromotive force V across the slit. The created capacitor allows a current $I = i\omega CV$ to flow through the ring even if it is discontinuous. In essence, the split-ring is an LC-resonator, and the Faraday law $i\omega\Phi + V = 0$ explains it by linking the capacitive and inductive contributions.

Our goal is to find the permeability μ_{eff} of the effective medium that approximates best the actual metamaterial. The equivalent homogeneous medium behavior is completely defined by it's constitutive electromagnetic parameters. This electromagnetic approach should lead to a resonance of μ_{eff} to match to LC-resonator nature of the split-ring.

Given the cell periodicity, all the electromagnetic parameters and the magnetic fields are C-periodic. So for each vector τ in the Bravais lattice $\mathcal{T} = \{\sum_i \tau_i V_i, \tau_i \in Z\}$. The permeability is invariant $\mu(M+\tau) = \mu(M)$ by all translations of the group $\mathcal{T}$, so the problem to solve $\mathcal{P}$ is to find a linear relation $B = \mu_{eff} H$ between the averages

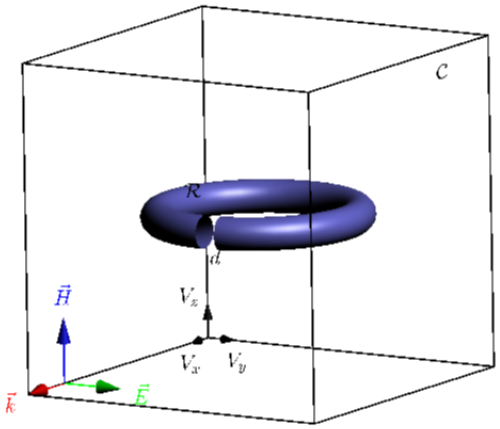

FIG. 1. The cubic unit cell $\mathcal{C}$ generated by an orthonormal base $\{V_x, V_y, V_z\}$, hosts a single metallic ring $\mathcal{R}$ of section Σ and split's width d. The equivalent capacitance is $C = \frac{\epsilon\Sigma}{d}$

of the fields over the cell $B = \langle b \rangle$ and $H = \langle h \rangle$:

$$|\mathcal{C}|\mu_{eff}(\omega)H \cdot H = \langle \mu|h^2| - \bar{\epsilon}|e^2| \rangle \tag{1}$$

Where $|\mathcal{C}|$ stands for the volume of the cell. The electric field e could be strong enough to let the effective permeability become negative. We should obtain a frequency dependent permeability, with negative values at the resonance.

B. An issue with the homogenization

The homogenization presented here follows the Bloch analysis idea. We take into account the conductivity in the permittivity formula $\epsilon = \epsilon_0\epsilon_r - i/(\sigma\omega)$. Let us write the Maxwell equations over the unit cell :

$$\begin{array}{c} -i\omega d + roth = j \\ i\omega b + rote = 0 \\ divd = q \quad divb = 0 \\ divj + i\omega q = 0 \\ d = \epsilon e \quad b = \mu h \end{array} \tag{2}$$

The Floquet-Bloch decomposition of a function φ consists in writing it as the sum of weighted functions $\hat{\varphi}_\kappa$ over the Brillouin zone $\mathcal{B}$, the dual of the unit cell $\mathcal{C}$, generated by the dual vectors $W^i V_j = 2\pi\delta_{ij}$:

$$\varphi(x) = (2\pi)^{-3} \int_{\mathcal{B}} exp(i\kappa \cdot x)\hat{\varphi}_\kappa(x) d\kappa \tag{3}$$

The Bloch modes $\hat{\varphi_\kappa}$ live in the unit cell $\mathcal{C}$ and are C-periodic. They are obtained by a discrete summation over $\mathcal{C}$:

$$\hat{\varphi}_\kappa(x) = |\mathcal{C}| \sum_{\tau \in \mathcal{T}} exp(-i\kappa\cdot(x+\tau))\varphi(x+\tau) \tag{4}$$

The Floquet-Bloch homogenization consists in throwing (3) into the equation to be solved. which results in a family of problems of the same kind, one for each κ. This is very helpful when we have a single wavelength vector κ. It could seem strange in our case to replace a differential equation by an infinite set of equations. Nevertheless, the homogenization process permits to solve the new set of the problems indexed by κ in one stroke.

We begin by applying the Bloch analysis to the full Maxwell equations. We notice that the curl and divergence operators become $(rot + i\kappa\times)$ and $(div + i\kappa\cdot)$. The new problem $\mathcal{P}$ is for each κ :

$$\begin{array}{c} -i\omega\hat{d}_\kappa + (rot + i\kappa\times)\hat{h}_\kappa = \hat{j}_\kappa \\ i\omega\hat{b}_\kappa + (rot + i\kappa\times)\hat{e}_\kappa = 0 \\ (div + i\kappa\cdot)\hat{d}_\kappa = \hat{q}_\kappa \quad (div + i\kappa\cdot)\hat{b}_\kappa = 0 \\ \hat{b}_\kappa = \mu\hat{h}_\kappa \quad \hat{d}_\kappa = \epsilon\hat{e_\kappa} \end{array} \tag{5}$$

The homogenization consists in shrinking the unit cell $\mathcal{C}$ to a point, hence expanding the Brillouin zone $\mathcal{B}$ to occupy the whole space. To study this limit, we will work in a homothety of the symmetry cell $\mathcal{C}_\alpha$, of size αa.

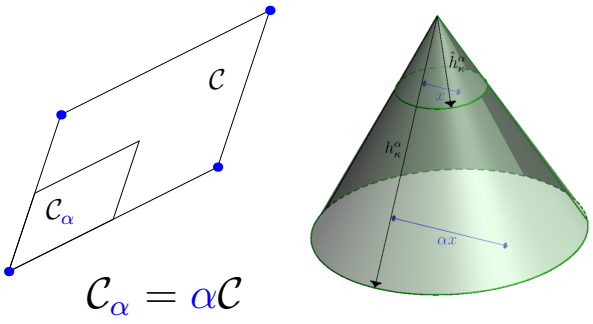

(a)Shrunk unit cell $\mathcal{C}_\alpha$ (b)Fields scaling

FIG. 2. Scaling operation

It has been proved[31] that the weighted averages of φ^α converges weakly to φ when $\alpha \to 0$. The exploitation of the unit cell smallness (homogenization hypothesis) comes by embedding this problem $\mathcal{P}$ in a family of problems $\mathcal{P}^\alpha_\kappa$ with a periodic permeability over C_α. The scaling transformation $h^\alpha_\kappa(x) = \hat{h^\alpha_\kappa}(\alpha x)$ is needed to pull-back to problem $\mathcal{P}^\alpha_\kappa$ into C, and therefore, we are able to compare $\mathcal{P}^\alpha_\kappa$ for a fixed κ and different $\alpha's$. So we finally have :

$$\begin{array}{c} -i\omega\alpha\hat{d}^\alpha_\kappa + (rot + i\kappa\alpha\times)\hat{h}^\alpha_\kappa = \alpha\hat{j}^\alpha_\kappa \\ i\omega\alpha\hat{b}^\alpha_\kappa + (rot + i\alpha\kappa\times)\hat{e}^\alpha_\kappa = 0 \\ (div + i\alpha\kappa\cdot)\hat{d}^\alpha_\kappa = \alpha\hat{q}^\alpha_\kappa \quad (div + i\alpha\kappa\cdot)\hat{b}^\alpha_\kappa = 0 \\ \hat{b}^\alpha_\kappa = \mu\hat{h}^\alpha_\kappa \quad \hat{d}^\alpha_\kappa = \epsilon\hat{e}^\alpha_\kappa \end{array} \tag{6}$$

The weak limit when $\alpha \to 0$ of the previous problem gives a value of the effective permeability but with disappointing results. In fact, the obtained electromagnetic parameters are the static one, with no frequency dependency.

$$\begin{array}{c} -i\omega\hat{d}_\kappa + i\kappa\times\hat{h}_\kappa = \alpha\hat{j}_\kappa \\ i\omega\hat{b}_\kappa + i\kappa\times\hat{e}_\kappa = 0 \\ div\hat{b}_\kappa = 0 \quad rot\hat{h}_\kappa = 0 \\ \hat{b}_\kappa = \mu_{eff}\hat{h}_\kappa \quad \hat{d}_\kappa = \epsilon_{eff}\hat{e}_\kappa \end{array} \tag{7}$$

C. From the split-ring to a closed ring

An ingenious solution to this problem comes by introducing a second small parameter[31], which competes with the structure period a. In the case of the split ring resonator, this small parameter is the slit's width $d \ll a \ll \lambda$. It becomes null faster than the symmetry cell period. The choice of the slit's width as a second small parameter can be explained by the LC-resonator analogy. The resonance condition $LC \sim \omega^2$ must be maintained during the homogenization and still an invariant feature for all the problems $\mathcal{P}^\alpha$. The capacity C and the induction L evolves like α, so the resonance is lost when the unit cell is shrunk ($\alpha \to 0$). By taking a slit's width that acts like $\alpha^3 d$, we obtain a capacity $C \sim \Sigma/d$ that behaves in $1/\alpha$ and are able to maintain the resonance. This particular choice of the problem $\mathcal{P}^\alpha$ is discussed in[35]. Taking into account the second hypothesis leads to :

$$\begin{aligned} \int_{\mathcal{C}^\alpha - \mathcal{R}} i\omega h^\alpha h' + \int_{\mathcal{C}^\alpha - \mathcal{R}} (i\omega\epsilon)^{-1}(roth^\alpha - j)roth' \\ + \int_{\Sigma^\alpha} (i\omega\epsilon)^{-1}\alpha^3 d(\vec{n}\cdot roth^\alpha)(\vec{n}\cdot roth') = 0 \end{aligned} \tag{8}$$

Once the Bloch transformation and the scaling applied, we obtain :

$$\begin{aligned} &\alpha^3 \int_{\mathcal{C}-\mathcal{R}} i\omega h^\alpha h' \\ &+ \alpha \int_{\mathcal{C}-\mathcal{R}} (i\omega\epsilon)^{-1}((rot + i\alpha\kappa)h^\alpha - \alpha j)(rot + i\alpha\kappa)h' \\ &+ \alpha^3 \int_{\Sigma} (i\omega\epsilon)^{-1}\alpha^3 d(\vec{n}\cdot(rot + i\alpha\kappa)h^\alpha)(\vec{n}\cdot(rot + i\alpha\kappa)h') \end{aligned} \tag{9}$$

We clearly see that the new final term in α^3 maintains the balance between the capacitive and inductive influences. The second term implies a null curl of the vector field $\vec{h}$ everywhere in the unit cell.

When this material is immersed in a periodic uniform field H, a current I flows in the ring across the surface Σ. And because $\vec{\nabla}\times\vec{h}=0$, a multivalued magnetic potential φ exists as $\vec{h}=\vec{\nabla}(\varphi)$. To maintain the right value for the circulation of the field h follonwing the path $\mathcal{L}$ Fig.3, we introduce a cutting surface S through which the magnetic potential φ has a jump $[\varphi]$. According to Ampere's law, this jump equals the current $[\varphi]=I$. Also, we choose to close the ring and model the slit by a surface $\Sigma\vec{n}$ that bears a capacitive layer :

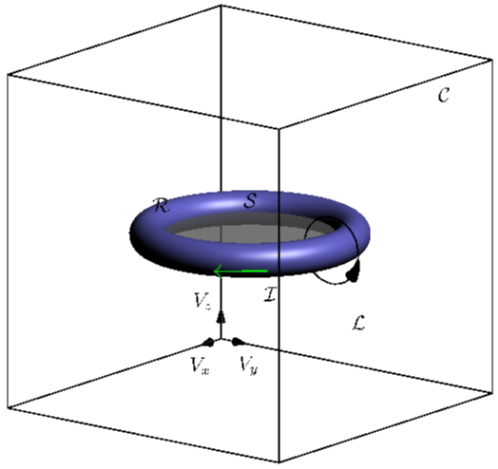

FIG. 3. Closed metallic ring with a cutting surface S

The main result of Ref.[31] is the weak formulation of this electromagnetic problem that also take into account the losses :

$$\int_{\mathcal{C}-\mathcal{R}}\mu\vec{\nabla}\varphi\cdot\vec{\nabla}\varphi'+\int_{\partial\mathcal{R}}\frac{1-i}{\sigma\omega\delta}\vec{\nabla}_S\varphi\cdot\vec{\nabla}_S\varphi'-\frac{1}{C\omega^2}[\varphi][\varphi'] = \int_{\mathcal{C}-\mathcal{R}}\mu\vec{H}\cdot\nabla\varphi' \quad (10)$$

Notice that even if the ring conductivity is finite, we choose to model losses effects by considering that the ring's skin $\partial\mathcal{R}$ bears a lossy layer. Once the potential φ found everywhere in the unit cell, we can compute the permittivity μ_{eff} of the orthotropic equivalent material:

$$\int_{\mathcal{C}-\mathcal{R}}\mu|\vec{\nabla}\varphi|^2+\int_{\partial\mathcal{R}}\frac{1-i}{\sigma\omega\delta}|\vec{\nabla}_S\varphi|^2-\frac{1}{C\omega^2}I^2 = |\mathcal{C}|,H\mu^*_{eff}H \quad (11)$$

The imaginary part of the permeability is clearly negative, while the real part becomes negative after the resonance frequency. The complex effective permeability in the tree directions of the lattice is a 3x3 diagonal dyadic $\mathcal{T}.\mu_{eff}=diag(\mu_{xx},\mu_{yy},\mu_{zz})$. For instance, if the orientated cutting surface $\vec{S}$ is collinear to V_z, we only need the value of $\mu_{zz}(\omega)$, obtained for $H=V_z$ from equation (11). The permeability dyadic is in this case:

$$\mu_{eff}(\omega)=\begin{bmatrix}\mu_0\mu_r & 0 & 0\\ 0 & \mu_0\mu_r & 0\\ 0 & 0 & \mu_{zz}(\omega)\end{bmatrix} \quad (12)$$

III. DISCRETIZATION

We have to take into account the periodicity of the unit cell when we mesh it. Therefore, each opposite faces of the unit cell are identically meshed.

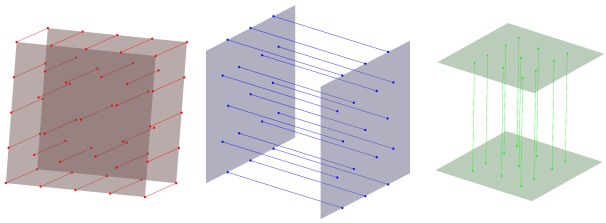

(a)$\vec{V_x}$ periodicity (b)$\vec{V_y}$ periodicity (c)$\vec{V_z}$ periodicity

FIG. 4. Identified pairs of nodes on the unit cell's opposite faces

Also, because the behavior of the resonant ring is described by the cutting surface S and the skin depth δ, it becomes unnecessary to mesh inside the ring. Finally, we know that the potential has a jump through the surface S. We can model this phenomenon by doubling the nodes on the surface S. For each node N_{s+} of the surface S, we will add to the mesh another node N_{s-} having the coordinates of N_{s+}. N_{s-} is connected to the tetrahedral elements located "under" the cutting surface S while N_{s+} will be only connected to the tetrahedrons "above" S.

The initial mesh and the geometry are created with a Comsol script program which allows to choose the dimensions, the orientation and the ring geometry. Then, another program transforms the mesh, by detecting the nodes correspondence between the opposite faces of the unit cell and by doubling the nodes on the cutting surface S.

We use nodal finite elements associated to the elementary functions λ_i, to solve the previous weak formulation. We have to solve a matrix equation $M\varphi=L$. The magnetic potential on each node of the mesh φ is the vector unknown and M the stiffness Hermitian matrix :

$$M_{ij}=\int_{\mathcal{C}-\mathcal{R}}\mu\vec{\nabla}\lambda_i\cdot\vec{\nabla}\lambda_j+\int_{\partial\mathcal{R}}\frac{1-i}{\sigma\omega\delta}\vec{\nabla}_S\lambda_i\cdot\vec{\nabla}_S\lambda_j - \frac{1}{C\omega^2}\lambda_I\lambda'_I \quad (13)$$

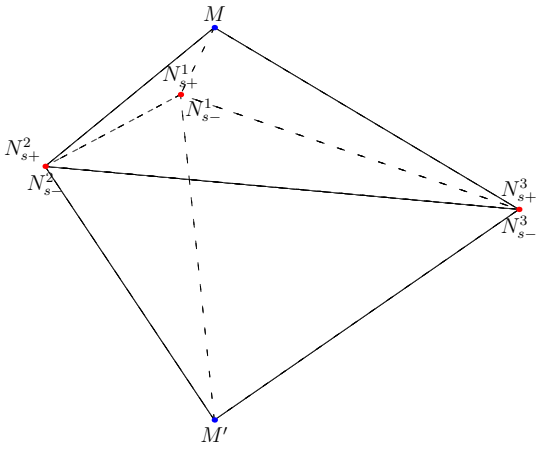

FIG. 5. Node doubling on the cutting surface S.

$$L_i = \int_{\mathcal{C}-\mathcal{R}} \mu \vec{H} \cdot \nabla \lambda_i \tag{14}$$

In fact, several equations link the components of the unknown vector φ. We have constant difference $\{C_x, C_y, C_z\}$ of magnetic potential between the unit cell opposite faces:

$$\forall i \quad \begin{array}{l} \varphi^i_{x=\alpha} - \varphi^i_{x=0} = C_x \\ \varphi^i_{y=\alpha} - \varphi^i_{y=0} = C_y \\ \varphi^i_{z=\alpha} - \varphi^i_{z=0} = C_z \end{array} \tag{15}$$

Besides, the following equation links the unknowns on the doubled nodes of the surface S with the current I:

$$\forall i \; \varphi^i_{s+} - \varphi^i_{s-} = I \tag{16}$$

We have to eliminate the vector unknowns $\varphi_{x=\alpha}$, $\varphi_{y=\alpha}$, $\varphi_{z=\alpha}$ and φ_{s+}, then compute the values of the four constant unknowns C_x, C_y, C_z and I as well as the value of the potential on the remaining nodes.

At this point, it is necessary to change the nodes order to solve the matrix equation while taking into account these constraints. The nodes should be reordered to have the following unknowns vector : $\varphi = [\varphi_r, \varphi_{x=0}, \varphi_{y=0}, \varphi_{z=0}, \varphi_{s+}, \varphi_{x=a}, \varphi_{y=a}, \varphi_{z=a}, \varphi_{s-}]$. We place all the remaining nodes at the beginning of the vector, those who are not on the faces of the unit cell nor on the cutting surface S.

The new system that correspond to an unknown vector $\varphi = [\varphi_r, \varphi_{x=0}, \varphi_{y=0}, \varphi_{z=0}, \varphi_{s+}, C_x, C_y, C_z, I]$ could be described by a simpler case studied in the Appendix.

IV. RESULTS AND DISCUSSION

A. Numerical results

Several simulations have been made for different orientations, ring's dimensions, slit's width and conductivity. In this paper, most of the simulations are made on the torus $\mathcal{T}^3_2$. It has a slit's width of $d = 0.1mm$, an internal radius $r_{int} = 2mm$ and an external redius $r_{ext} = 3mm$. We choose air as a host medium and a period of 1cm. The resonance is obtained at 8.18 GHz. The skin depth δ is ensured to be much smaller than the slit's width d to maintain a coherent model of the ring.

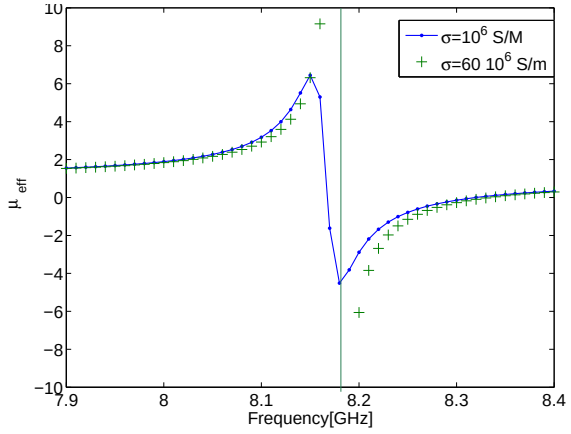

(a)Effective relative permeability function of the frequency (Ghz)

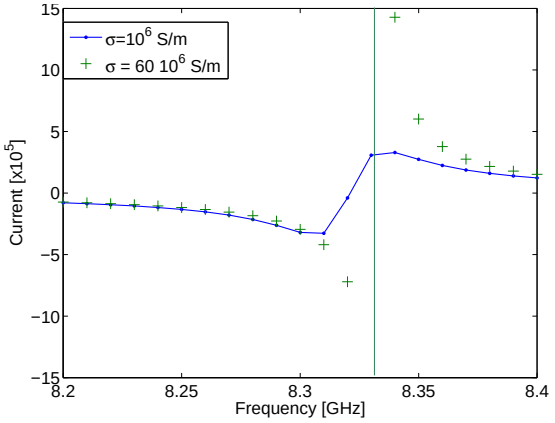

(b)Curent (A) function of the frequency (Ghz)

FIG. 6. Simulation of the structure T^3_2 with $\sigma = 60\,10^6\,S/m$ (blue) and $\sigma = 10^6\,S/m$ (green)

The current and the relative effective permeability diverge at the resonance if we consider a perfect conductor. When the losses are taken into account by considering a finite ring conductivity, the simulations show that the resonance frequency slightly decreases when the split-ring is less conductive. The losses decreases with the ring's conductivity, and the real part of the effective permittivity is smaller at the resonance when the ring is less

conductive.

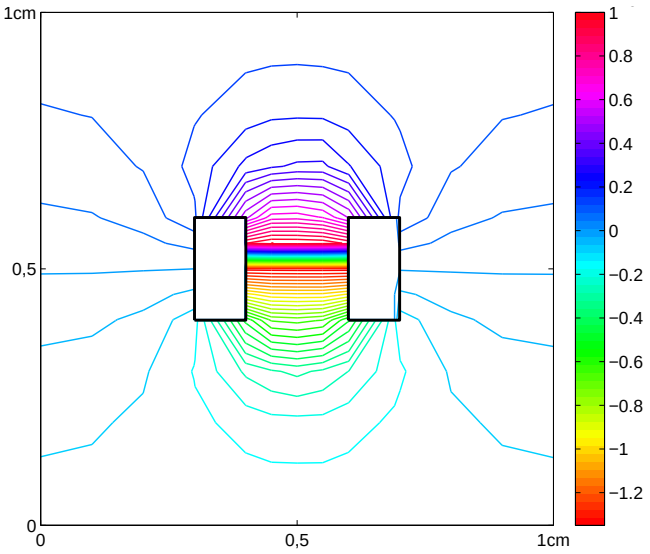

FIG. 7. Magnetic isopotentials in a vertical slice of the unit cell

Studying the isopotentials Fig.7 is necessary to determine a map of the electromagnetic field inside the metamaterial. The isopotentials are drawn on the vertical slice that contains the center of the unit cell. The potential has only been computed on the mesh's nodes, so, the barycentric coordinates are used to interpolate the value of the magnetic potential on each point of the slice. The isopotentials have shown a potential "jump" through the cutting surface $\int$. As $\vec{h}$ is orthogonal to the isopotentials, it seems that the major part of the magnetic field flows through the cutting surface S.

B. Dimensions effect

The split ring is in essence an LC-circuit, for which we have a resonance at the frequency $LC\omega_0^2 = 1$. We can deduce the influence if several parameters from this very simple principle and confirm the validity of our simulations.

The capacity is inverse proportional to the slit's width, and the equivalent inductance is completly independent from this parameter. Therefore, the resonance frequency $f_0 \sim \sqrt{d}$ is proportional to the square root of the slit's width, which is consistent with the simulations Fig.8(a).

The magnetic energy in the cell essentially depends on the flux on the magnetic field through the curring surface $\mathcal{S}$. The equivalent inductance $L \sim \pi r_{int}^2$ is then proportional to the area of $\mathcal{S}$. In the other hand, the capacity is proportional to the slit's area $C \sim \Sigma = \pi(r_{ext} - r_{int})^2/4$. We find a final dependency of the resonance frequency in $f_0 \sim ((r_{ext} - r_{int})r_{int})^{-1}$, which agrees very well with the dependency profile that our simulations give 8(b)

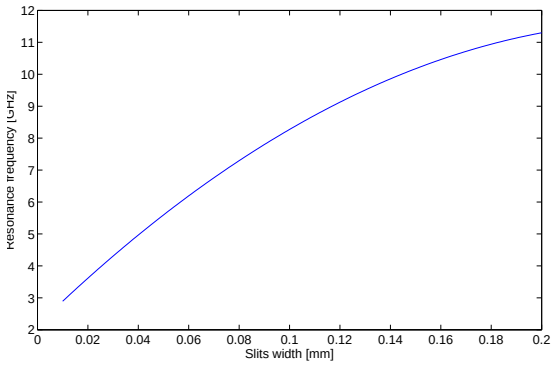

(a)Resonance frequency (GHz) function of the slit's width (mm)

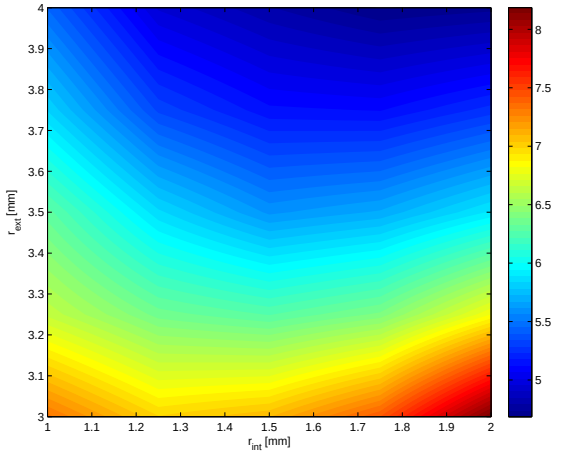

(b)Resonance frequency (GHz) function of the internal and external radius (mm)

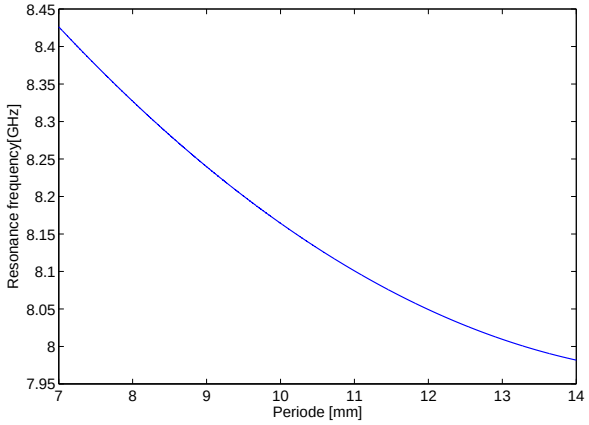

(c)Resonance frequency (GHz) function of the unit cell size (mm)

FIG. 8. Influence of the split-ring array dimensions

The impact of the array period on the resonance frequency is much weaker than those of the rings dimensions. A wider unit cell size means more magnetic energy in it, and therefore a reduction of the resonance frequency

8(c). But the influence of the cell size is weak because the magnetic potential flows essentially through the cutting surface $\mathcal{S}$.

C. An analytical effective permeability formula

We can also study 2D structures by extending the rings height to the unit cell size. The unit cell is then defined by three areas :

1. The interior region A_1, limited by the internal boundary of the ring, of area a_1 and where the magnetic field is $h = h_1$
2. The metallic ring R where $h = 0$.
3. The exterior region A_2, limited by the external boundary of the ring and the limits of the unit cell, of area a_2 and where $h = h_2$.

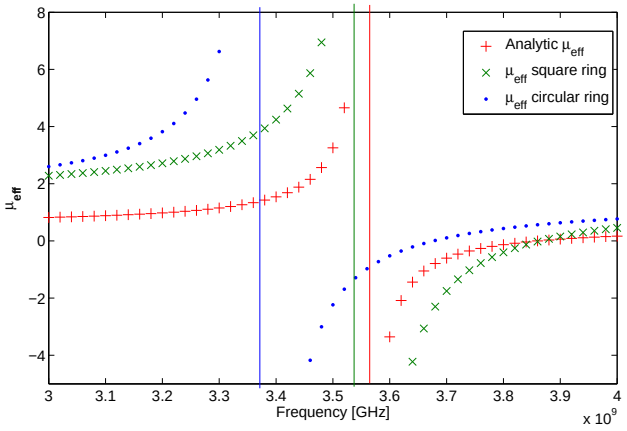

FIG. 9. Effective analytical and simulated permeability

By Ampere's law, $I = h_1 - h_2$ is the current that flows through the ring. By Faraday's law, the voltage drop across the gap $V = -i\omega\Phi$ is related to the magnetic flux Φ. This voltage drop is also the voltage across the capacitor conductors (the slit faces), so we have $I = i\omega CV$. These relations give the electromagnetic fields outside the ring :

$$h_1 = \frac{c\,\mu_{eff} H}{\mu_0(a_1 + a_2(1 - Ca_1\mu_0\omega^2))} = \frac{h_2}{1 - C\mu_0 a_1\omega^2} \quad (17)$$

The permeability is negative between the frequencies $\omega_1 = \frac{1}{\sqrt{Ca_1\mu_0}}$ and $\omega_2 = \sqrt{1 + \frac{a_1}{a_2}}\omega_1$:

$$\mu_{eff} = \mu_0 \frac{a_1 + a_2}{c} \frac{\left(\frac{\omega}{\omega_2}\right)^2 - 1}{\left(\frac{\omega}{\omega_1}\right)^2 - 1} \quad (18)$$

Far from the resonance, the material is supposed to behave as a diamagnetic one. In fact, the ring's acts like an obstacle to the magnetic flux, which is weaker than the flux in an empty elementary cell.

The effective permeability of circular and square rings have been computed and compared to the analytical one Fig.9. The areas $a_1 = 9mm^2$ and $a_2 = 51mm^2$ are the same in the three cases to have a common basis of comparison. The simulations shows a very good agreement with the formula (18). While the resonance frequency with the analytical law give 3.57 GHz, the circular and square rings resonate at 3.38 and 3.54 GHz. The agreement is better for the square ring because the constant field hypothesis would less describe the magnetic field in the case of circular contours.

The asymptotes near the resonance of the analytical law do not match those of the simulated curve because we assumed constant fields in the areas A_1 and A_2. However, the frequency window where the permeability has a negative real part is clearly consistent with the analytical results even with the constant fields simplifying hypothesis.

D. Free space measurments

We compare in this section the measured resonance frequency of an array of circular split-rings to the results of the simulations and the analytical law Eq.18. The measurements are done in free space with two horn antennas (2–18 GHz), focused with Rexolite lenses. The focused beam is considered as Gaussian, so we ensure that the incident wave is planar, at least in the narrow region where we put the metamaterial to be measured.

The PNA S-parameters have to be calibrated before we have the proper S-parameters. To achieve the TRL (*Thru*, *Line*, *Reflect*) calibration procedure, we use a two port model correction. Therefore, we need to move the second horn antenna by the thickness of the metal plate (*Reflect*). Micrometric positioning fixtures are used to move precisely the antennas along the propagation axis.

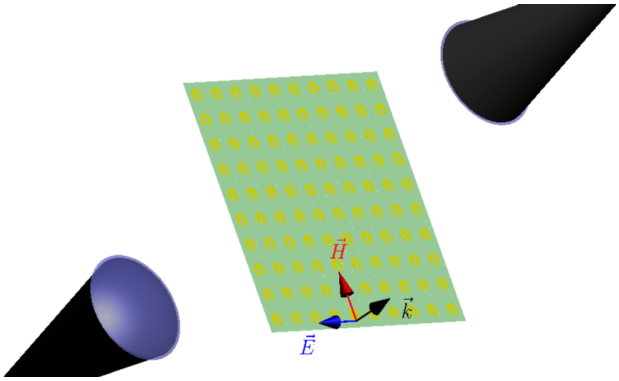

FIG. 10. Free space characterisation of an epoxy slab hosting copper rings

However, the calibration procedure is not sufficient to eliminate the multiple reflections noise. We apply a gating in the time domain, which greatly reduce the noise, but make the S-parameters ring in the frequency domain. We show here the measures of a split-ring array of copper rings hosted in epoxy ($\epsilon_r = 4.8$). The sample is 1.6 mm thick in the propagation direction, and 20x20 cm^2 wide in a transverse plane. The unit cell is 1cm large and contains a copper ring of internal radius $r_{int} = 1mm$, external radius $r_{ext} = 2.5mm$ and slit's width is 1mm. These dimensions have been chosen to obtain a resonance near 10GHz. Our purpose is to avoid the limits of the range 2–18 GHz because the ringing phenomena induced by the gating make the S-parameters less precise there.

We choose to characterize this metamaterial with a perpendicular polarization, for which the magnetic field is transverse to the rings. It is quite different from the parallel polarization that we used in our simulations, but it appears from Ref.[11] that the resonance frequency is the same in the two cases .

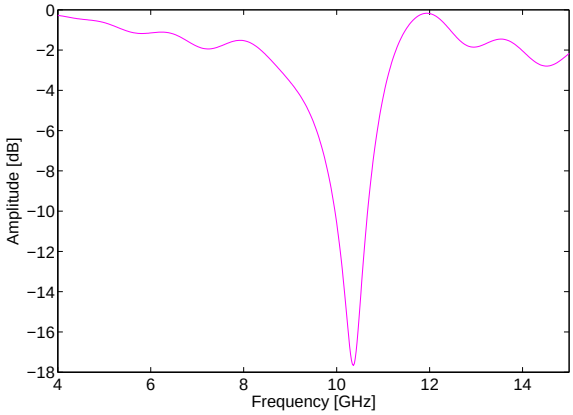

(a) Magnitude dB

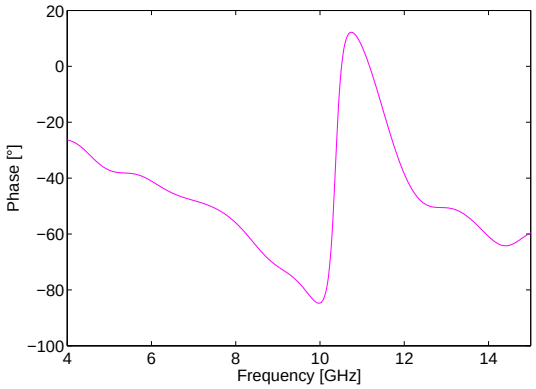

(b) Phase °

FIG. 11. S_{21} measured parameters in free space

This sample have a measured resonance frequency of 10.36 GHz. The simulations and the analytical law give respectively 10.19 GHz and 10.1 GHz. Hence, we obtain a very good agreement.

V. CONCLUSION

We have successfully computed by homogenization the frequency dependent permeability of split-ring arrays. We were able to solve the encountered issues when one try to homogenize metamaterials with resonant inclusions. By its original transformation of the single split-ring by a closed ring, this method provides a computation of the effective permeability at a minimal cost. Besides, the simulator structure and effectiveness offers a simple way to optimize these metamaterials shapes and dimensions.

The influences of the ring dimensions are predicted by simple physical arguments, that consists in replacing this metamaterial with it's equivalent LC circuit. The correctness of our method is verified by comparing numerical, analytical and measured results for bidimensional structures. The simulations are in fact more precise than the analytical law and they predict the resonance frequency with a relative error of 1.6%.

However, the slit's relative position doesn't play any role in a closed ring effective permeability. A possible model of the capacitive layer Σ by edge finite elements would properly take into account it's position and describe the displacement currents through the slit. This evolution of our model would permit to simulate the unit cells containing multiple split rings.

Appendix: Solving a Hermitian system with constraints

In this appendix, we show through a simple case how to transform a hermitian matrix equation to take into account a constraint over the unknown vector. Suppose that we want to solve the following system $AX = B$. The matrix A being hermitian ($^T\bar{A} = A$), it is defined by six block matrices :

$$\begin{bmatrix} A_{11} & A_{12} & A_{13} \\ {}^t\bar{A}_{12} & A_{22} & A_{23} \\ {}^t\bar{A}_{13} & {}^t\bar{A}_{23} & A_{33} \end{bmatrix} \begin{bmatrix} x \\ y \\ z \end{bmatrix} = \begin{bmatrix} b_1 \\ b_2 \\ b_3 \end{bmatrix} \qquad (A.1)$$

Suppose that a constraint $z_i - y_i = C$ applies to all the elements of the vectors y and z. To get rid of these redundant unknowns, we multiply the equation sides by the vector ${}^t\bar{X}$ and then substitute the z vector components by $z_i = y_i + C$. The brand new hermitian matrix

equation to solve is $A'^t[xyC] = B'$, with.

$$A' = \begin{bmatrix} A_{11} & A_{12}+A_{13} & \sum_j A_{13}^{ij} \\ A_{21}+A_{31} & A_{22}+2A_{23}+A_{33} & \sum_j A_{23}^{ij} + A_{33}^{ij} \\ \sum_i A_{31}^{ij} & \sum_i A_{32}^{ij} + A_{33}^{ij} & \sum_i \sum_j A_{33}^{ij} \end{bmatrix} \begin{bmatrix} b_1 \\ b_2+b_3 \\ \sum_i b_3^i \end{bmatrix} \tag{A.2}$$

ACKNOWLEDGMENTS

It is a pleasure to acknowledge our helpful discussions with Alain Bossavit and his efficient support in the implementation of this method.

* said.zouhdi@supelec.fr

[1] C. Simovski and S. He, Physical Letters A **311**, 254 (2003).
[2] H. Chen, L. Ran, J. Huangfu, X. Zhang, K. Chen, T. M. Grzegorczyk, and J. A. Kong, Phys. Rev. E **70**, 057605 (2004).
[3] V. Veselago, Soviet Physics Uspekhi **10**, 509 (1968).
[4] K. B. Alici and E. Ozbay, Journal of Applied Physics **101**, 083104 (2007).
[5] P. A. Belov, Y. Hao, and S. Sudhakaran, Phys. Rev. B **73**, 033108 (2006).
[6] J. B. Pendry, Phys. Rev. Lett. **85**, 3966 (2000).
[7] J. B. Pendry, A. J. Holden, D. J. Robbins, and W. J. Stewart, Journal of Physics: Condensed Matter **10**, 4785 (1998).
[8] J. Pendry, A. Holden, D. Robbins, and W. Stewart, IEEE Transactions on Microwave Theory and Techniques **45**, 2075 (1999).
[9] A. Radkovskaya, M. Shamonin, C. J. Stevens, G. Faulkner, D. J. Edwards, E. S. E., and L. Solymar, Microwave and optical technology letters **46**, 474 (2005).
[10] K. Aydin and E. Ozbay, Physica status solidi. B. Basic research **244**, 1197 (2007).
[11] P. Gay-Balmaz and O. J. F. Martin, Journal of applied physics **92**, 2929 (2002).
[12] J. García-García, F. Martín, J. D. Baena, R. Marqués, and L. Jelinek, Journal of Applied Physics **98**, 033103 (2005).
[13] D. R. Smith, S. Schultz, P. Markos, and C. M. Soukoulis, Phys. Rev. B **65**, 195104 (2002).
[14] W. Weir, Proc. IEEE **62**, 33 (1974).
[15] X. Chen, T. M. Grzegorczyk, B.-I. Wu, J. Pacheco, Jr., and J. A. Kong, Phys. Rev. E **70**, 016608 (2004).
[16] A. Bensoussan, J. Lions, and G. Papanicolaou, *Asymptotic methods for periodic structures* (North Holland, 1978).
[17] A. Sihvola, *Electromagnetic mixing formulas and applications*, IEE Electromagnetic Waves Series, Vol. 47 (IEE, 1999).
[18] P. A. Belov and C. R. Simovski, Phys. Rev. E **72**, 026615 (2005).
[19] D. R. Smith and J. B. Pendry, Journal of the Optical Society of America B **23**, 391 (2006).
[20] O. Acher, J.-M. Lerat, and N. Malléjac, Opt. Express **15**, 1096 (2007).
[21] D. R. Smith, J. J. Mock, A. F. Starr, and D. Schurig, Phys. Rev. E **71**, 036609 (2005).
[22] G. Allaire, SIAM Journal on Mathematical Analysis **23**, 1482 (1992).
[23] D. Cioranescu, A. Damlamian, and G. Griso, SIAM journal on mathematical analysis **40**, 1585 (2008).
[24] M. Belyamoun and S. Zouhdi, in *Electromagnetics in Advanced Applications, 2009. ICEAA '09. International Conference on*, IEEE Conferences, Vol. 1898 (2009) pp. 952–953.
[25] G. Allaire and C. Conca, Journal de Mathmatiques Pures et Appliqus **77**, 153 (1998).
[26] D. Sjöberg, C. Engström, G. Kristensson, D. Wall, and N. Wellander, Multiscale Modeling and Simulation **4**, 149 (2005).
[27] M. Gorkunov, M. Lapine, E. Shamonina, and K. Ringhofer, The European Physical Journal B - Condensed Matter and Complex Systems **28**, 263 (2002), 10.1140/epjb/e2002-00228-4.
[28] M. Silveirinha, Phys. Rev. B **75**, 115104 (2007).
[29] M. Silveirinha, J. Baena, L. Jelinek, and R. Marqués, Metamaterials **3**, 115 (2009), metamaterials-2008 Congress in Pamplona: Electromagnetic characterization of Metamaterials.
[30] J. D. Baena, L. Jelinek, R. Marqués, and M. Silveirinha, Phys. Rev. A **78**, 013842 (2008).
[31] A. Bossavit, IEEE Transactions on Magnetics **45**, 1276 (2009).
[32] J. Pendry, A. Holden, D. Robbins, and W. Stewart, IEEE Trans. Microwave Theory Tech. **47**, 2075 (1999).
[33] R. Marqus, F. Medina, and R. Rafii-El-Idrissi, Phys. Rev. B **65**, 144440 (2002).
[34] R. Marqus, F. Mesa, J. Martel, and F. Medina, IEEE Trans. Antennas Propagat. **51**, 2572 (2003).
[35] S. Zouhdi, A. Sihvola, and M. Arsalane, "Advances in electromagnetics of complex media and metamaterials," (Kluwer (Dordrecht), 2009) p. 89.